Autonomous Alignment of Peg and Hole by Force/Torque Measurement for Robotic Assembly*

Te Tang[1], Hsien-Chung Lin[1], Yu Zhao[1], Wenjie Chen[2] and Masayoshi Tomizuka[1]

Abstract— In the past years, many methods have been developed for robotic peg-hole-insertion to automate the assembly process. However, many of them are based on the assumption that the peg and hole are well aligned before insertion starts. In practice, if there is a large pose(position/orientation) misalignment, the peg and hole may suffer from a three-point contact condition where the traditional assembly methods cannot work. To deal with this problem, this paper proposes an autonomous alignment method by force/torque measurement before insertion phase. A three-point contact model is built up and the pose misalignment between the peg and hole is estimated by force and geometric analysis. With the estimated values, the robot can autonomously correct the misalignment before applying traditional assembly methods to perform insertions. A series of experiments on a FANUC industrial robot and a H7h7 tolerance peg-hole testbed validate the effectiveness of the proposed method. Experimental results show that the robot is able to perform peg-hole-insertion from three-point contact conditions with 96% success rate.

I. INTRODUCTION

Peg-hole-insertion, i.e., inserting a round peg into a round hole, is a common task in assembly process. In the past several years, many methods have been developed for robotic peg-hole-insertion. There are passive methods, such as remote center compliance (RCC [1]), and active methods, such as impedance control [2], admittance control [3] and hybrid force/velocity control [4]. The general idea is to make the system compliant to the environment and to modify the nominal trajectory on-line to minimize contact force during assembly.

Fig. 1 shows the four possible alignment conditions before insertion begins. From left to right, they are 'line contact', 'one-point contact', 'two-point contact' and 'three-point contact', respectively. Many robotic peg-hole-insertion methods focus on the insertion phase and assume that the peg and hole are already well aligned. Those methods work well only if the initial configuration is one of the first three contact conditions [5]. Insertion with a three-point contact is quite difficult because three degrees of freedom of the peg with respect to the hole are constrained. Therefore, there is little space left for the robot control algorithm to compliantly insert the peg into the hole.

If the assembly environment is well structured, i.e., the peg and hole's poses are known in advance, then it is not difficult

[1]Department of Mechanical Engineering, University of California, Berkeley, CA, USA. {tetang,hclin, yzhao334, tomizuka}@berkeley.edu

[2]Learning Robot Department, Robot Laboratory, FANUC Corporation, Japan. wjchen@berkeley.edu
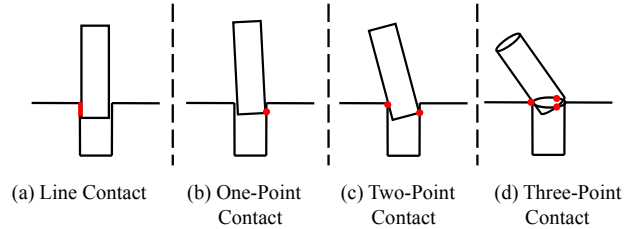
Fig. 1. Four alignment conditions between peg and hole before insertion.

to generate a suitable trajectory to align the two mating parts accurately. However, in many cases the environment is unstructured. For example, in a human-robot-collaboration (HRC) scenario [6], the pose of the hole is unknown to the robot. The human operator guides the robot arm via lead-through-teaching mode to align the peg coarsely towards the hole. It is highly possible that insertion starts with the three-point contact condition. Note that in Fig. 1(d), the tilt angle is exaggerated for the ease of illustration. In practice, the three-point contact may appear more frequently compared to the other three conditions, especially in high precision industrial tasks where even a small tilt angle can result in a three-point contact.

There are several works that address the peg hole alignment problem in different ways. In [7] and [8], the pose of the hole was estimated by vision feedback and the autonomous alignment was realized by visual servoing. However, these vision based methods require additional vision sensors, which increase the system cost and complexity. Moreover, the hole's orientation is estimated by the normal vector of the surface around the hole. This involves making an implicit assumption that the hole is perpendicular to its surrounding surface, which is not always the case [9]. [10] and [11] performed the peg hole alignment by force control. They first adjusted the peg's orientation by pressing the peg's free end flushed against the hole surface and then randomly slid the peg on the surface to eliminate position misalignment. However, this method also requires the hole to be perpendicular to its surface and random search may make the cycle time long.

To deal with these problems, a new peg hole alignment method based on geometric and force analysis is proposed in this paper. It utilizes force/torque (F/T) sensor measurement to estimate the relative pose from the peg to the hole under the three-point contact condition. Based on the pose estimation, a compensation movement is generated and applied to directly eliminate the peg hole misalignment. This method

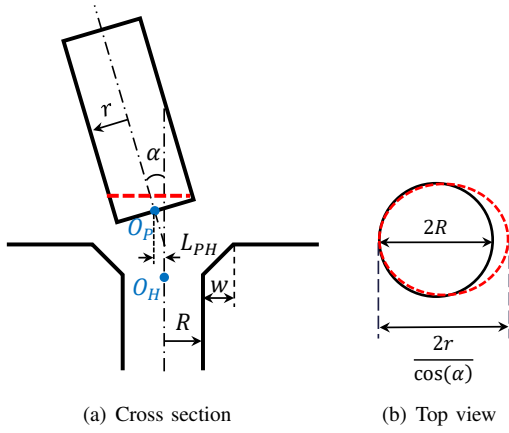(a) Cross section   (b) Top view

Fig. 2. Schematic diagram of peg hole insertion.

does not require vision sensors, sliding on the surface, and also does not require the hole to be perpendicular to its surrounding surface. Therefore, the proposed method is non-costly, efficient and robust.

The remainder of this paper is organized as follows: Section II discusses the three-point contact in details and the requirements to avoid three-point contact. Section III introduces the geometric and force analysis of the three-point contact model, from which the closed form equations for the relative pose from peg to hole are derived. An optimization formulation is also introduced to estimate the friction coefficient. In Section IV, a series of experiments are performed on FANUC LR Mate 200*i*D/7L [12] to show the effectiveness of the proposed method. The robot succeeded in peg-hole-insertion from three-point contact condition with 96% success rate. The supplementary videos can be found at [13]. Section V concludes the paper and proposes future works.

II. ANALYSIS OF INITIAL CONTACT CONDITIONS

Fig. 2(a) shows the cross section of the peg and hole, where R is the hole radius, r is the peg radius, and α is the tilt angle between peg axis and hole axis. Denote the center point of the peg's end face as O_P, and the center point of the hole as O_H. Note that if the hole is chamfered with width w, then O_H is not on the surface of the hole, but below the surface. The lateral distance between O_P and O_H along the hole's radius direction is denoted as L_{PH}.

The misalignment between peg and hole is defined by position misalignment (L_{PH}) and the orientation misalignment (α). The peg would contact the chamfer instead of the surrounding surface if the following equation is satisfied,

$$L_{PH} < R - r\cos(\alpha) + w \tag{1}$$

With the compliance that robot provides (either by passive methods or active methods), if the peg contacts the chamfer first, it could then slide along the chamfer and finally make contact with the hole. Equation (1) highlights the importance of chamfer. $R - r\cos(\alpha)$ on the right hand side is typically a small number compared to chamfer width w. Therefore, the

additive w term relaxes the difficulty in position alignment for assembly.

Suppose the peg has slid along the chamfer and finally contacts the hole, then the orientation misalignment (α) will determine which initial contact condition (see Fig. 1) will occur. As shown in Fig. 2, the peg's cross section, marked by the red dashed line, is projected to the hole's surface plane. The length of the projected ellipse's major axis is $2r/\cos(\alpha)$. Three-point contact occurs if and only if

$$\frac{2r}{\cos(\alpha)} > 2R \tag{2}$$

Equation (2) can be rewritten as

$$\alpha > \cos^{-1}\left(\frac{r}{R}\right) \tag{3}$$

which indicates that if the tilt angle is larger than a threshold, the three-point contact will occur. The smaller the clearance between peg and hole, the lower the threshold.

The following section will introduce how to compute the estimated lateral distance $\widehat{L}_{PH}$ and the estimated tilt angle $\widehat{\alpha}$ from contact forces and torques. Then the robot can apply a compensation movement from these estimates to eliminate pose misalignment. From (1) and (3), if the estimation errors of $\widehat{L}_{PH}$ and $\widehat{\alpha}$ are bounded by

$$\|\widehat{L}_{PH} - L_{PH}\| < R - r\cos(\alpha) + w \approx w \tag{4}$$

$$\|\widehat{\alpha} - \alpha\| < \cos^{-1}\left(\frac{r}{R}\right) \tag{5}$$

then the residue L_{PH} and α after compensation are small enough to get out of the three-point contact state. Experimental results in Section IV will show that the proposed method's estimation errors satisfy the above bounds.

III. AUTONOMOUS ALIGNMENT ANALYSIS

This section will derive the relative pose from peg to hole by force analysis and geometric analysis, assuming that the peg and hole are in a three-point contact condition.

A. Force Analysis

As shown in Fig.3, the Cartesian coordinates $x^P - y^P - z^P$ are attached to the peg center point O_P, where z^P is parallel to the peg axis, and x^P is selected such that the peg and hole are symmetric about the $x^P - z^P$ plane. Among the three contact points, denote the one on the peg's cylindrical surface by P_c, and the other two symmetric points on the end face by P_{e1} and P_{e2}. On contact point P_c, the normal force applied to the peg is F_c along x^P axis, and the friction force is μF_c along z^P axis, where μ is the friction coefficient. On contact points P_{e1} and P_{e2}, the normal force is F_e along z^P axis, and the friction force is μF_e along x^P axis [14].

The forces on the three contact points generate resultant forces F_x, F_z and torque M_y on center point O_P, with

$$F_x = F_c + 2\mu F_e \tag{6}$$

$$F_z = \mu F_c + 2F_e \tag{7}$$

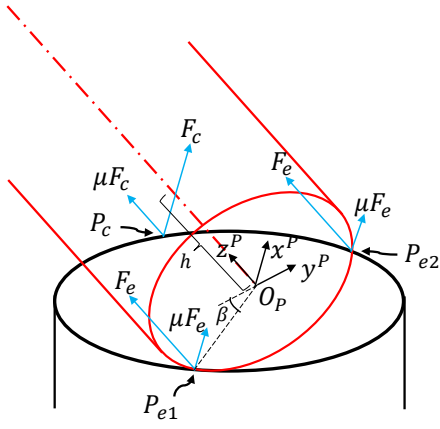$$M_y = F_c h + \mu F_c \cdot r + 2F_e \cdot r\sin(\beta) \tag{8}$$

Fig. 3. Force Analysis of three-point-contact

where h denotes the distance between P_c and O_P along z^P, and β denotes the angle between $\overrightarrow{O_P P_{e1}}$ and y^P.

F_x, F_z and M_y can be measured by the F/T sensor equipped at the robot end-effector. If μ is known, then F_e and F_c become

$$F_e = \frac{F_z - \mu F_x}{2(1 - \mu^2)} \tag{9}$$

$$F_c = \frac{F_x - \mu F_z}{1 - \mu^2} \tag{10}$$

Substitute (9) and (10) into (8) to get

$$\mu^2(rF_z - M_y) + \mu\{hF_z + [\sin(\beta) - 1]rF_x\} + [M_y - hF_x - \sin(\beta)rF_z] = 0 \tag{11}$$

Equation (11) can be furthur simplified to

$$M_y - hF_x - \sin(\beta)rF_z = 0 \tag{12}$$

if $\mu \approx 0$.

Equations (11) and (12) indicate that h and β form an equality constraint with the force/torque measurement values. The following geometric analysis will show that h and β are both functions of tilt angle α, which leads to the closed form expression of α.

B. Geometric Analysis

Similar to the above analysis, another Cartesian coordinates $x^H - y^H - z^H$ are set up and attached to the hole center point O_H, with z^H along the hole axis and y^H parallel to the y^P. Note that the peg and hole in Fig. 4 are supposed to be in contact, but the peg in the figure is lifted virtually for the ease of coordinates illustration.

The transformation matrix from the hole coordinates to the peg coordinates is

$$T_P^H = \begin{bmatrix} \cos(\alpha) & 0 & -\sin(\alpha) & \Delta O_x^H \\ 0 & 1 & 0 & \Delta O_y^H \\ \sin(\alpha) & 0 & \cos(\alpha) & \Delta O_z^H \\ 0 & 0 & 0 & 1 \end{bmatrix} \tag{13}$$
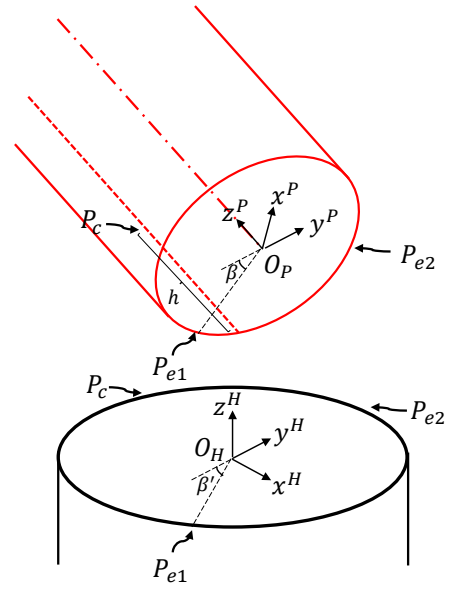

Fig. 4. Geometric Analysis of three-point-contact

where $[\Delta O_x^H, \Delta O_y^H, \Delta O_z^H]^T$ is the position of O_P in the hole coordinates.

The three contact points P_c, P_{e1} and P_{e2} can be described by the two coordinate frames [5]:

$$P_c^P = \begin{bmatrix} -r & 0 & h & 1 \end{bmatrix}^T \tag{14}$$

$$P_{e1}^P = \begin{bmatrix} -r\sin(\beta) & -r\cos(\beta) & 0 & 1 \end{bmatrix}^T \tag{15}$$

$$P_{e2}^P = \begin{bmatrix} -r\sin(\beta) & r\cos(\beta) & 0 & 1 \end{bmatrix}^T \tag{16}$$

$$P_c^H = \begin{bmatrix} -R & 0 & 0 & 1 \end{bmatrix}^T \tag{17}$$

$$P_{e1}^H = \begin{bmatrix} R\sin(\beta') & -R\cos(\beta') & 0 & 1 \end{bmatrix}^T \tag{18}$$

$$P_{e2}^H = \begin{bmatrix} R\sin(\beta') & R\cos(\beta') & 0 & 1 \end{bmatrix}^T \tag{19}$$

The above six vectors should satisfy the following constraints,

$$P_c^H = T_P^H \cdot P_c^P \tag{20}$$

$$P_{e1}^H = T_P^H \cdot P_{e1}^P \tag{21}$$

$$P_{e2}^H = T_P^H \cdot P_{e2}^P \tag{22}$$

Substitute (14)-(19) into (20)-(22) to get the expressions of β and h with respect to α,

$$h = \frac{2R - 2r\cos(\alpha)}{\sin(\alpha)} \tag{23}$$

$$\beta = \sin^{-1}\left(\frac{r\cos^2(\alpha) - 2R\cos(\alpha) + r}{r\sin^2(\alpha)}\right) \tag{24}$$

Furthermore, the position offset between the two origins O_P and O_H can be derived in the hole frame,

$$\Delta O_x^H = R - r\cos(\alpha) \tag{25}$$

$$\Delta O_y^H = 0 \tag{26}$$

$$\Delta O_z^H = \frac{r\cos^2(\alpha) - 2R\cos(\alpha) + r}{\sin(\alpha)} \tag{27}$$

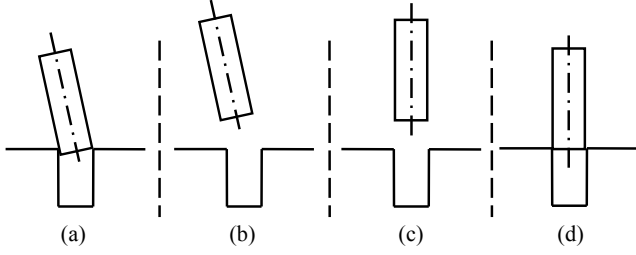Fig. 5. Trajectory to compensate the misalignment between peg and hole.

	inch (UI)	mm (SI)	Tolerance
Hole	$1.000^{+0.0001}_{-0.0000}$	$25.400^{+0.003}_{-0.000}$	H7
Peg	$0.999^{+0.0000}_{-0.0002}$	$25.370^{+0.001}_{-0.000}$	h7

C. Autonomous Alignment by Compensation

Substituting (23) and (24) into (11), we arrive at an equation with α as the only unknown variable

$$(F_z - \mu F_x)\left[r\cos^2(\alpha) - 2R\cos(\alpha) + r\right]$$
$$+ 2(F_x - \mu F_z)\sin(\alpha)(R - r\cos(\alpha))$$
$$= \left[(rF_z - M_y)\mu^2 - rF_x\mu + M_y\right]\sin^2(\alpha) \qquad (28)$$

In practice, the radius of peg and hole are very close, otherwise the peg could be loosely inserted and there is no need to apply peg alignment. By assuming $R \approx r$, then the following simplified closed form expression for α is obtained,

$$\alpha = 2\tan^{-1}\left(-\frac{F_x - \mu F_z}{F_z - \mu F_x}\right.$$
$$\left.+ \frac{\sqrt{r^2(F_x - \mu F_z)^2 + r(F_z - \mu F_x)[(rF_z - M_y)\mu^2 - rF_x\mu + M_y]}}{r(F_z - \mu F_x)}\right) \qquad (29)$$

which describes the orientation misalignment between peg and hole in the three-point contact condition.

Because it is easier to program the robot end-effector's movement in the tool coordinates, (25)-(27) are transformed to obtain the position of O_H in the peg coordinates,

$$\Delta O_x^P = R\cos(\alpha) - r \qquad (30)$$
$$\Delta O_y^P = 0 \qquad (31)$$
$$\Delta O_z^P = \frac{R\cos^2(\alpha) - 2r\cos(\alpha) + R}{\sin(\alpha)} \qquad (32)$$

which represent the position misalignment between peg and hole in the three-point contact condition.

With these misalignment estimations, a compensation trajectory can be generated to eliminate the misalignment. Fig. 5 shows one possible trajectory that was designed in this work. Starting from the three-point contact condition, the robot first backs the peg back along the peg axis (Fig. 5(b)), then adjust the peg's pose such that it is accurately aligned above the hole (Fig. 5(c)). This adjustment takes place in the air in order to avoid collision. Finally, the robot feeds the peg straight down towards the hole until contact (Fig. 5(d)). With this compensation, the three-point contact would be effectively eliminated and the peg is aligned to the hole with line contact, one-point contact or two-point contact conditions. Then traditional assembly methods can be used for insertion.

D. Estimation of Friction Coefficient

Estimating the tilt angle α by (29) requires the friction coefficient μ between peg and hole. The nominal friction coefficient between two materials is easy to get from reference. However, in practice, the friction coefficient is influenced by the shape, size, and chamfer of the mating parts on top of the material type. This subsection introduces a method to estimate the friction coefficient if unknown.

From (29), the tilt angle is estimated by a nonlinear function

$$\widehat{\alpha} = f(\mu, m) \qquad (33)$$

with μ and m as variables, where m are the measurement values from F/T sensor. In experiment, suppose we already know the accurate pose of the peg and hole, then the real tilt angle is known. By comparing the real α and the estimated $\widehat{\alpha}$, the friction coefficient can be regressed by solving the following optimization problem

$$\mu^* = \arg\min_{\mu}\ \sum_{i=1}^{n}\|\alpha_i - \widehat{\alpha}_i\|^2 \qquad (34)$$
$$s.t.\quad \widehat{\alpha}_i = f(\mu, m_i)$$

Since the constraint is highly nonlinear, there is no guarantee for a global minimum. The nominal friction coefficient can be utilized as the initial value in order to get an acceptable local minimum.

IV. EXPERIMENT

To demonstrate the performance of the proposed alignment method, a series of experiments were performed on an industrial robot, FANUC LR Mate 200iD/7L [12]. Experimental video can be found at [13].

The testbed is shown in Fig. 6. The peg and hole were both machined from Aluminium 6061-T6, with a peg diameter of 0.999in (25.370mm), a hole diameter of 1.000in (25.400mm) and 1.0mm chamfers. The assembly tolerance is industry standard H7h7 (see Table I). An ATI Mini45 F/T sensor [15] is embedded in the robot end-effector to measure the force and torque during assembly.

The first part of the experiment is designed to estimate the friction coefficient μ. The hole is fixed with a known pose as well as having its axis aligned with the vertical line. The peg is grasped and pushed towards the hole with a three-point contact configuration by the robot. The pushing force is around 10N along the $-z^P$ direction and 30N along the $-x^P$ direction. The peg is tilted at four known angles, $10.36°, 15.75°, 20.38°, 26.47°$, and the corresponding
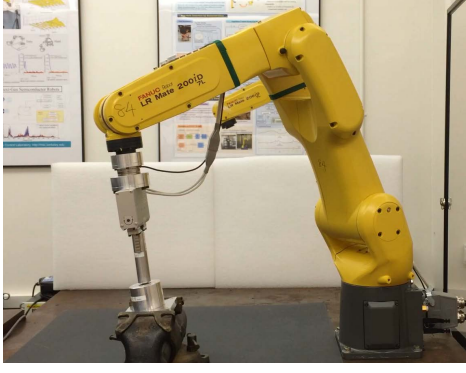
Fig. 6. Peg-Hole-Insertion Testbed. The diameters of peg and hole are 25.370mm and 25.400mm respectively, with 0.030mm clearance (H7h7 tolerance). The model of industrial robot is FANUC LRMate-200*i*D/7L.
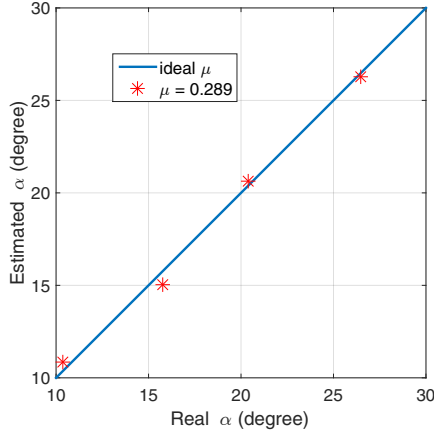

Fig. 7. Estimated tilt angles in four calibration measurements.

Fig. 8. Estimated tilt angles from force/torque measurements.

force/torque measurements are recorded at these four configurations. The friction coefficient μ is estimated by solving the nonlinear optimization (34) by MATLAB Optimization Toolbox [16] with initial value $\mu^0 = 0.4$ [17]. The optimal solution is $\mu^* = 0.289$. As shown in Fig. 7, the estimated tilt angles using μ^* are $10.86°, 15.02°, 20.63°, 26.28°$ respectively, which are all close to the aforementioned actual tilt angles.

After μ is estimated, the second part of the experiment is performed to estimate the pose misalignment between peg and hole. In this experiment, the hole is randomly placed by the human operator. The robot has no prior information on the pose of the hole. By lead through teaching mode, the human operator guides the robot arm to approach the peg to contact the hole. Then the robot switches to force control mode, and autonomously applies constant force to push the peg to maintain close contact. The pushing force is around 10N along the $-z^P$ direction and 30N along the $-x^P$ direction. Forces/torques are measured and then the tilt angle (α) as well as the hole center position (O_H relative to O_P) are estimated respectively by (29)-(32).

As discussed in Section II, there will be errors in the misalignment estimations. However, if the estimation errors
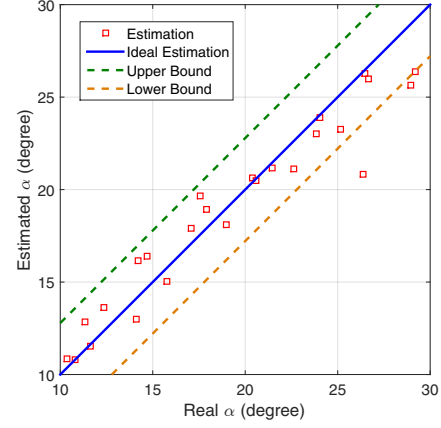
are bounded by (4) and (5), the peg and hole will no longer be in three-point contact after compensation. For this specific testbed, the error bound for orientation estimation is $\cos^{-1}(25.370/25.400) = 2.785°$, and the error bound for position estimation is $w = 1mm$.

Fig. 8 shows the orientation estimation results. The horizontal axis denotes the real tilt angle, and the vertical axis represents the estimated tilt angle. In twenty five experiments, most of the orientation estimations are inside the error bounds ($\pm 2.785°$), except for one case which has a deviation of $-5.1°$. The average of absolute estimation errors is $1.248°$. One interesting observation is that these estimations are not evenly distributed around the ideal estimation line (blue line in Fig. 8). Estimations tend to be larger when $\alpha \in [10°, 20°]$ and to be smaller when $\alpha \in [20°, 30°]$. This trend can possibly be attributed to the fact that our estimation equation for orientation (29) utilizes a constant friction coefficient μ. In practice, however, the friction coefficient might vary if the tilt angle between peg and hole changes.

Fig. 9 shows the estimation results of the hole's position. The horizontal axis denotes the experimental index from 1 to 25. The vertical axis represents the position estimation error in the x^H direction in each experiment. The average of absolute estimation errors is $0.3546mm$. All of the position estimations are within the error bounds ($\pm 1mm$).

After the pose misalignment is estimated, a compensation trajectory is generated and performed by the robot to eliminate the misalignment (see Fig. 10(a)-(c)). It first pulls the peg back and then aligns the peg towards the hole in the free space. In Fig. 10(d), since the three-point contact has been ruled out, traditional hybrid force/velocity control is utilized here to insert the peg into the hole. In the twenty five experiments, robot successfully inserts the peg into the hole twenty four times (96% success rate). The only unsuccessful experiment fails because the residue tilt angle between peg and hole is larger than the error bound (see Fig. 8).

To conclude, the experimental results show that the proposed alignment method can accurately estimate the pose misalignment between peg and hole. The misalignment can
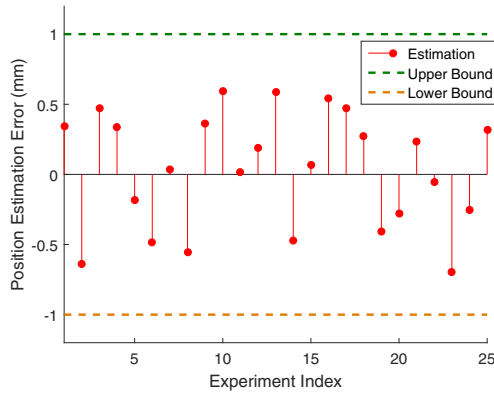
Fig. 9. Estimating hole's position from force/torque measurements.
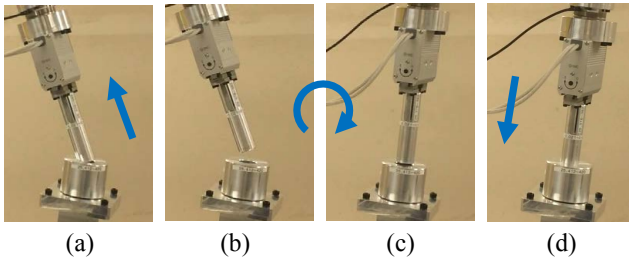

(a)   (b)   (c)   (d)

Fig. 10. Autonomous alignment procedure for peg hole insertion.

be effectively compensated by the designed compensation trajectory. After compensation, traditional assembly methods can be applied to insert the peg into the hole. This alignment method has many promising applications. For example, in the future assembly line, there is no need for the human to measure the hole's pose or program the robot an approaching trajectory. The human can roughly lead the robot to put mating parts into contact with each other, then the robot can autonomously correct the misalignment and perform assembly.

V. CONCLUSIONS

For peg-hole-insertion task in an unstructured environment, the peg and hole might suffer from a three-point contact condition, where traditional robotic assembly methods cannot work. To deal with this problem, an autonomous alignment method is proposed in this paper. The closed form equations for peg-hole misalignment are derived from a force and geometric analysis. A compensation trajectory is designed to realign the peg and hole to avoid three-point contact. The friction coefficient is estimated by nonlinear optimization and a series of experiments are performed to test the proposed method. Experimental results show that the misalignment between the peg and hole with H7h7 tolerance can be effectively eliminated and the robot can conduct peg-hole-insertion from three-point contact condition with 96% success rate. In the future, we will test the performance of this method on more peg-hole testbeds, with different materials, sizes and tolerances.

REFERENCES

[1] D. Whitney and J. Nevins, *What is the remote center compliance (RCC) and what can it do?* Charles Stark Draper Laboratory, 1978.
[2] D. E. Whitney, "Historical perspective and state of the art in robot force control," *The International Journal of Robotics Research*, vol. 6, no. 1, pp. 3–14, 1987.
[3] J. J. Craig, *Introduction to robotics: mechanics and control.* Pearson Prentice Hall Upper Saddle River, 2005, vol. 3.
[4] M. H. Raibert and J. J. Craig, "Hybrid position/force control of manipulators," *Journal of Dynamic Systems, Measurement, and Control*, vol. 103, no. 2, pp. 126–133, 1981.
[5] H. Bruyninckx, S. Dutre, and J. De Schutter, "Peg-on-hole: a model based solution to peg and hole alignment," in *Robotics and Automation, 1995. Proceedings., 1995 IEEE International Conference on*, vol. 2. IEEE, 1995, pp. 1919–1924.
[6] T. Tang, H.-C. Lin, and M. Tomizuka, "A learning-based framework for robot peg-hole-insertion," in *ASME 2015 Dynamic Systems and Control Conference*. American Society of Mechanical Engineers, 2015, pp. V002T27A002–V002T27A002.
[7] S. Huang, K. Murakami, Y. Yamakawa, T. Senoo, and M. Ishikawa, "Fast peg-and-hole alignment using visual compliance," in *Intelligent Robots and Systems (IROS), 2013 IEEE/RSJ International Conference on*. IEEE, 2013, pp. 286–292.
[8] S. Huang, Y. Yamakawa, T. Senoo, and M. Ishikawa, "Realizing peg-and-hole alignment with one eye-in-hand high-speed camera," in *Advanced Intelligent Mechatronics (AIM), 2013 IEEE/ASME International Conference on*. IEEE, 2013, pp. 1127–1132.
[9] N. Asakawa, K. Toda, and Y. Takeuchi, "Automation of chamfering by an industrial robot; for the case of hole on free-curved surface," *Robotics and Computer-Integrated Manufacturing*, vol. 18, no. 5, pp. 379–385, 2002.
[10] S. R. Chhatpar and M. S. Branicky, "Search strategies for peg-in-hole assemblies with position uncertainty," in *Intelligent Robots and Systems, 2001. Proceedings. 2001 IEEE/RSJ International Conference on*, vol. 3. IEEE, 2001, pp. 1465–1470.
[11] M.-O. Hongler, F. Badano, M. Betemps, and A. Jutard, "A random exploration approach for automatic chamferless insertion," *The International journal of robotics research*, vol. 14, no. 2, pp. 161–173, 1995.
[12] FANUC America, LR Mate 200*i*D/7L, "http://robot.fanucamerica.com /products/robots/productbyseries.aspx?seriesid=3&robotseries=lr%20-mate%20series."
[13] Supplementary video for the paper, http://me.berkeley.edu/~tetang/ CASE2016/AutoAlignment.html.
[14] W. Haskiya, K. Maycock, and J. Knight, "Robotic assembly: chamferless peg-hole assembly," *Robotica*, vol. 17, no. 6, pp. 621–634, 1999.
[15] ATI Mini45 F/T sensor, "http://www.ati-ia.com/Products/ft."
[16] M. A. Branch and A. Grace, *MATLAB: optimization toolbox: user's guide version 1.5.* The MathWorks, 1996.
[17] M. Vukobratovic, V. Potkonjak, and V. Matijevic, *Dynamics of robots with contact tasks.* Springer Science & Business Media, 2013, vol. 26.